THE JOURNAL OF PHYSICAL CHEMISTRY LETTERS
A JOURNAL OF THE AMERICAN CHEMICAL SOCIETY

pubs.acs.org/JPCL Letter

Quantifying the Ligand-Induced Triplet Energy Transfer Barrier in a Quantum Dot-Based Upconversion System

Tsumugi Miyashita, Paulina Jaimes, Tianquan Lian,* Ming Lee Tang,* and Zihao Xu*

Cite This: J. Phys. Chem. Lett. 2022, 13, 3002−3007 Read Online

ACCESS | Metrics & More | Article Recommendations | Supporting Information

ABSTRACT: During photon upconversion, quantum dots (QDs) transfer energy to molecules in solution through a long ligand shell. This insulating ligand shell imparts colloidal stability at the expense of efficient photosensitization. For the first time, we quantify the barrier these aliphatic ligands pose for triplet energy transfer in solution. Using transient absorption spectroscopy, we experimentally measure a small damping coefficient of 0.027 Å^{-1} for a ligand exceeding 10 carbons in length. The dynamic nature of ligands in solution lowers the barrier to charge or energy transfer compared to organic thin films. In addition, we show that surface ligands shorter than 8 carbons in length allow direct energy transfer from the QD, bypassing the need for a transmitter ligand to mediate energy transfer, leading to a 6.9% upconversion quantum yield compared with 0.01% for ligands with 18 carbons. This experimentally derived insight will enable the design of efficient QD-based photosensitizers for catalysis and energy conversion.

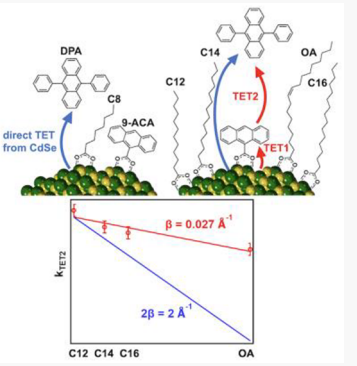

Photon upconversion[1−3] allows for advances in solar light harvesting[4] and deep tissue bioimaging.[5] It typically consists of many transfer steps; for example, QD sensitized photon upconversion involves two triplet energy transfer (TET) steps.[6,7] The first TET (TET1, blue arrow, Figure 1)

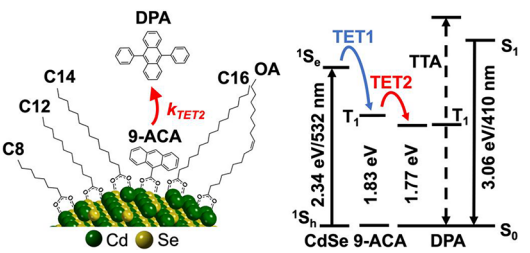

Figure 1. Triplet energy transfer from CdSe QDs with carboxylic acid ligands of different length to 9-anthracene carboxylic acid (9-ACA) transmitter ligand (TET1) and then from 9-ACA to the 9,10-diphenylanthracene (DPA) emitter (TET2).

step occurs from the photoexcited QD to the surface bound mediator molecule, and the second TET (TET2, red arrow, Figure 1) from the mediator to the emitter in the solution. Previous studies have focused mainly on TET1, where effects of QD size,[8,9] quality,[6,10] mediator structure,[6,11,12] solvent,[1] temperature,[2,13] and so on have been explained. In contrast, there has been only one report on the TET2 step, which shows that its rate is not diffusion limited, contrary to previous assumptions.[6] Here, we focus on TET2 to develop a deeper understanding for further improving upconverting nanomaterials.

Understanding the TET2 step is important to engineer QD-based photon upconversion for deep tissue imaging. Bottlenecks in TET2 will dictate the rational design of oil-in-water micelles where the efficient diffusion of excitons for TTA is required.[14] In retrospect, the fact that the rate of TET2 (k_{TET2}) was 3 orders of magnitude slower than the diffusion limited value for the PbS QD light absorber/tetracene mediator/rubrene emitter system should not be surprising, since the rubrene acceptor has to navigate the long, greasy oleic acid ligands anchored on the PbS to reach the tetracene mediator.[6] Motivated to investigate this further, using nanosecond transient absorption (ns-TA) spectroscopy, we measured k_{TET2} in a three-component photoconversion system consisting of CdSe QD light absorbers, 9-anthracene carboxylic acid (9-ACA) mediators and 9,10-diphenylanthraccene (DPA) and rubrene emitters. We find that the k_{TET2} in this system is on the same order of magnitude as PbS QDs for CdSe QDs with long surface ligands, but short ligands allow fast direct triplet transfer from the QD photosensitizer. In fact, CdSe with short octanoic acid ligands can directly photosensitize DPA for a 6.9% upconversion quantum yield (UCQY) without the need for a surface-bound transmitter ligand. Under the same conditions, oleic acid-capped CdSe have a low UCQY of ∼0.01%. Our ns-TA data shows that by decreasing the length

Received: February 20, 2022
Accepted: March 23, 2022
Published: March 29, 2022

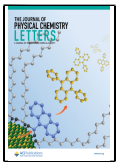

https://doi.org/10.1021/acs.jpclett.2c00514
J. Phys. Chem. Lett. 2022, 13, 3002−3007

Table 1. Key Parameters for the Study of k_{TET2} of CdSe Nanocrystals with Different Lengths of Carboxylic Ligands for Photon Upconversion

X-CdSe/9-ACA with emitter in toluene (DPA: 5 mM; rubrene: 1 mM)	distance (Å)[a]	ave. 9-ACA[b]	τ_1 (ns)	τ_2 (μs)	τ_3 (ns)	k_{TET2} (μs^{-1})[c]	photon upconversion QY (%)[d]
C8-CdSe/9-ACA + DPA	9.56	14.2	8.96 ± 0.96	-	-	-	3.77
C12-CdSe/9-ACA + DPA	10.5	13.5	19.4 ± 1.40	2.15 ± 0.00	-	0.461	17.5
C14-CdSe/9-ACA + DPA	11.5	13.7	7.74 ± 0.61	2.57 ± 0.05	-	0.385	1.69
C16-CdSe/9-ACA + DPA	12.3	13.0	10.5 ± 0.49	2.74 ± 0.01	-	0.362	2.08
OA-CdSe/9-ACA + DPA	16.3	12.0	8.01 ± 0.20	3.27 ± 0.02	405.3 ± 29	0.302	18.1

[a]The QD-mediator distance is reported to be the length of the linearly extended carbons in the carboxylic acid ligands.[20] [b]The average number of molecules per QD, obtained from UV−vis absorbance spectra in Figure S2B. [c]Calculations described in SI section 5. [d]100% is defined as the emission of one high energy photon per two absorbed low energy photons (Eq S1).

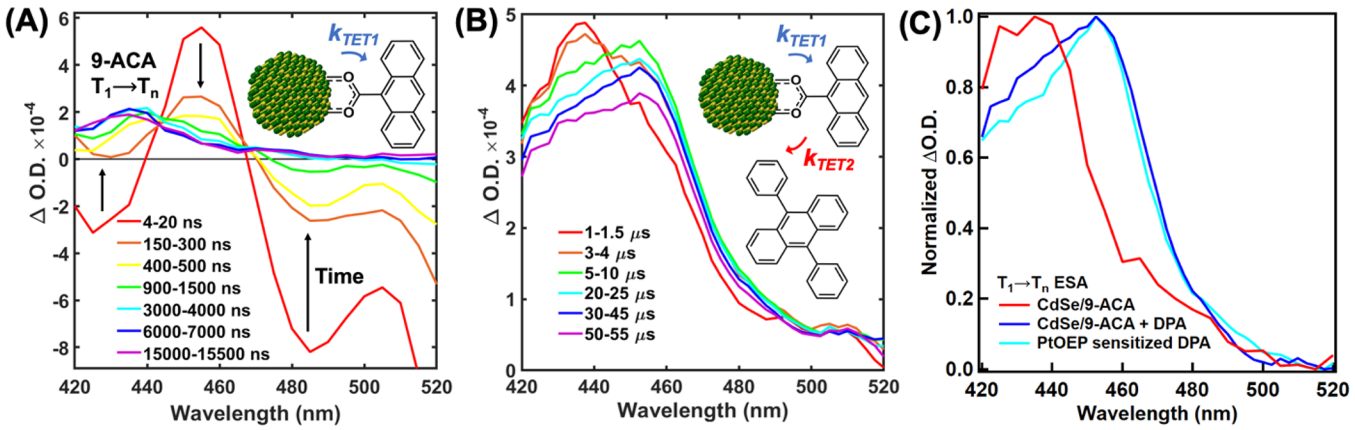

Figure 2. (A) Transient absorption (TA) spectra of oleic acid (OA)-CdSe/9-ACA hybrid nanomaterials. There is an isosbestic point at 468 nm. (B) TA spectra of the same OA-CdSe/9-ACA sample but dissolved in DPA (5 mM). Figure shows spectra from 1 to 55 μs delay time. (C) T_1 to T_n excited state absorption (ESA) spectra of the OA-CdSe/9-ACA at 50−50.5 μs in panel A (red), and the OA-CdSe/9-ACA with 5 mM DPA at 30−45 μs in panel B (blue). Also shown is the DPA T_1 to T_n ESA spectrum sensitized by PtOEP (cyan). All samples are in toluene excited at 532 nm at RT.

of the solubilizing aliphatic chains from 18 to 12 carbons, or replacing oleic acid with dodecanoic acid, k_{TET2} increases from 0.30 to 0.46 μs^{-1}, showing a shallow dependence on the ligand length. This shallow dependence yields an exponential decay constant of 0.027 $Å^{-1}$, indicating that the TET2 rate is dominated by the slow penetration of DPA into the aliphatic ligand shell such that 9-ACA and DPA are within the Dexter distance (<1 nm).[15] Previous work has only documented static and collisional electron transfer from QDs capped with their original long ligands.[16] For the first time, this work quantifies how long aliphatic chains on nanoparticles impede charge or energy transfer from photoexcited QDs.

In this work, the CdSe QD photosensitizers are first excited by 532 nm photons (Figure 1). This photogenerated exciton then migrates to surface-bound triplet mediators, to create the triplet excited state on the 9-anthracene carboxylic acid (9-ACA) mediator ligand. This is the first TET step (denoted as TET1, transfer rate as k_{TET1}). With long ligands exceeding 10 carbons, the TET2 (with rate of k_{TET2}) step then occurs from this 9-ACA ligand to DPA emitter molecules, which are excited to their lowest excited triplet state, or T_1 states. Two excited DPA emitters collide and undergo triplet−triplet annihilation (TTA), yielding one molecule in its singlet excited and the other in its ground state, S_1 and S_0, respectively. Emission from the DPA S_1 state produces the high-energy violet photons. As we will show with short octanoic acid ligands (C8, left of Figure 1), direct TET from CdSe to DPA occurs.

To study the effect of ligand length, the original oleic acid (OA) ligands bound to the CdSe QDs were replaced with shorter linear carboxylic acid ligands and the resulting CdSe QDs were then functionalized with 9-ACA. These linear carboxylic acid ligands, X, are octanoic acid, dodecanoic acid, tetradecanoic acid, and hexadecanoic acid with 8, 12, 14, and 16 carbons, respectively, and labeled C8, C12, C14, and C16 for clarity (Figure 1). These carboxylic acid ligands are shorter than the original oleic acid (OA/C18) ligands; for example, octanoic acid (C8) is approximately the same as 9-ACA in length. Following Olshansky et al.'s ligand exchange procedure, we stirred the carboxylic acid ligands of variable length with the original OA-CdSe nanocrystals in toluene overnight at 100 °C. After they are cleaned, the CdSe with shorter carboxylic acid ligands (X-CdSe, X = C8, C12, C14, C16) are dissolved in toluene (Figure S1A/Section 1.4 in the Supporting Information (SI)).[17] In line with previous NMR experiments showing CdSe is capped with oleate ligands at a surface density of 4.5 nm^{-2},[18] NMR shows there are originally around 50 OA ligands per 2.7 nm diameter CdSe QD (Table S1). After ligand exchange, there are 120−230 aliphatic ligands per CdSe QD. This includes both surface-bound ligands and ligands in dynamic equilibrium with the surface in solution.[19] Then, the 9-ACA ligand is added to the QD surface as a transmitter ligand to produce X-CdSe/9-ACA, X = C8, C12, C14, C16, OA (Figure S1B). UV−vis absorption spectroscopy was used to calculate the average number of surface-bound 9-ACA ligands. As can be seen in Table 1, there are about an average of 13−14 9-ACA ligands bound on the CdSe QD.

Photon upconversion occurs when the X-CdSe/9-ACA hybrid complexes are excited by 532 nm light from a CW

https://doi.org/10.1021/acs.jpclett.2c00514
J. Phys. Chem. Lett. 2022, 13, 3002−3007

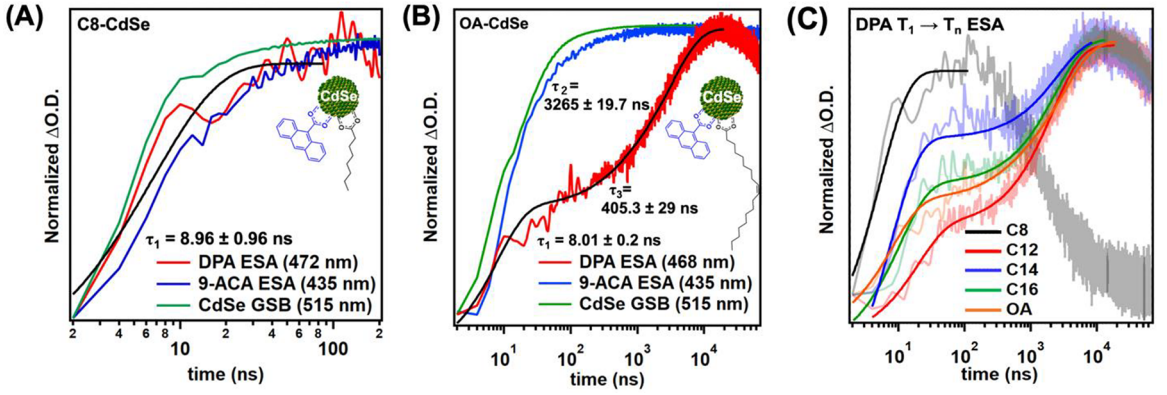

Figure 3. Transient kinetics of (A) C8-CdSe/9-ACA and (B) OA-CdSe/9-ACA with and without DPA. The kinetics of CdSe GSB (green) and 9-ACA ESA (blue) were monitored at 515 and 435 nm, respectively, in QD/9-ACA samples without the DPA emitter. The kinetics of DPA ESA (red) were monitored in samples containing DPA at 472 nm for C8-CdSe/9-ACA and 468 nm for OA-CdSe, which are isosbestic points that contain only DPA ESA signal. Fits to these kinetics (model described in SI Section 5) are shown in black lines. (C) Comparison of the normalized DPA ESA kinetics in QD samples with carboxylic acid ligands of different lengths obtained at each isosbestic point (Table 1). Ligands with more than 12 carbons show two TET2 time constants.

laser in the presence of 3 mM DPA, resulting in violet light being produced via triplet−triplet annhilation (Figure 1 and Figure S1C). Initially, we postulated that the decrease in QD solubilizing chain length would lead to a higher efficiency of energy transfer as the tunneling barrier for TET is reduced with shorter ligands.[9] However, experimentally, we observed that there is no trend in the photon upconversion upconversion (UCQY) with respect to ligand length (Table 1). UCQY values depend strongly on the purity of the newly introduced carboxylic acid ligands and the presence of surface defects introduced during the ligand exchange process.[10] In this work, the OA-CdSe/9-ACA in DPA sample has the highest UCQY at 18.1%. The UCQY is high for C12-CdSe/9-ACA at 17.5% but low for C8-CdSe/9-ACA at 3.77%. This is because surface defects are inadvertently introduced as the 100 °C ligand exchange temperature is not sufficient to repair the dangling bonds. However, a high UCQY is not the objective in this study since k_{TET2} is independent of k_{TET1}, and both k_{TET1} (TET rate from CdSe to 9-ACA) and k_{TET2} (TET rate from CdSe surface bound 9-ACA to DPA) can be measured directly via TA spectroscopy.

Nanosecond TA measurements were conducted to measure k_{TET1} and k_{TET2}. The X-CdSe/9-ACA complexes were excited by a pulsed YAG laser at 532 nm, the absorption maxima of CdSe, where the 9-ACA and DPA emitter does not absorb (Figure S1A). As shown in Figure 2A, the TA spectra of OA-CdSe/9-ACA in toluene initially show bleaches of the ground state absorption bands (GSBs) of CdSe centered at 425, 485, and 520 nm (Figure S1A), which monitor the population of excited QDs.[21] From ∼5 ns to ∼1000 ns, the excited state absorption (ESA) of the 9-ACA triplet at ∼435 nm grows, while the CdSe GSBs decay because of TET1 and intrinsic decay processes. When OA-CdSe/9-ACA is dissolved in 5 mM DPA/toluene solution, the DPA T_1 to T_n ESA is observed at later delay times (e.g., from 5−55 μs), as shown in Figure 2B. The DPA triplet ESA, centered at 460 nm, is red-shifted compared to 9-ACA, centered at 435 nm, as shown in Figure 2C. The former matches well with the DPA ESA spectra measured with PtOEP triplet sensitizers. Similar features are also observed in the ns-TA spectra of C8-CdSe/9-ACA and C12-CdSe/9-ACA in DPA (Figure S2). Note that there is an isosbestic point ∼470 nm between the QD and 9-ACA TA features. Since the signal at the ∼470 nm isosbestic point is zero at early times and the DPA triplet ESA dominates at this wavelength where the contribution from 9-ACA is small, we argue that the TA signal here reflects TET2. In the same way, isosbestic points of all other samples are chosen (Table S2). The TA signal at this wavelength contains only the DPA triplet absorption, allowing the measurement of k_{TET2} (see SI Section 3).

We measured k_{TET2} from X-CdSe/9-ACA, X = C8, C12, C14, C16, OA to DPA emitters at each isosbestic point shown in Table S2 using ns-TA spectroscopy. Unexpectedly, the TA data show two TET2 time constants when the aliphatic ligands exceed 10 carbons in length. TET2 rates can be fit from the kinetics at the CdSe QD exciton bleach, the 9-ACA transmitter ESA and the DPA annihilator ESA, monitored at 515, 435, and ∼470 nm, respectively (see Table S2 for the isosbestic points). The kinetics of CdSe QD and 9-ACA ligand were measured in QD/ACA samples without the DPA emitter to avoid the overlap of DPA and ACA ESA signals (Figure 2C). As shown in Figure 3 and S4, for all samples, the concurrent recovery of the CdSe GSB (green lines) and growth of the 9-ACA ESA at 435 nm (blue lines) show that TET1 occurs in one step directly from the CdSe donor to the surface bound 9-ACA acceptor. The measured τ_1, which includes both TET1 and CdSe decay processes, matches previous reports.[12,22] Compared with C8 (Figure 3A), for C12, C14, C16 and OA, the DPA triplet state grows in two distinct steps with time constants τ_1 and τ_2 (Figure 3B, 3C and S4). τ_1 is on the order of ns and shows no ligand dependence (similar to the time scale of instrument response, Figure S6), while τ_2 increases from C12 to C18 (Table 1). The desired k_{TET2} values can be obtained from τ_2 (SI Section 5, Figures S4, S5).

For the C8-CdSe/9-ACA + DPA sample, the DPA ESA grows on the same time scale as CdSe decay or 9-ACA growth (Figure 3A). This suggests direct TET from the CdSe to DPA, TET that competes with TET1 from the QD to the mediator. This growth in the DPA ESA suggests that some DPA molecules might intercalate in the hydrophobic ligand shell and are thus poised to receive triplets from the surface of CdSe. In order to confirm this intriguing observation, we measured the upconversion QY for CdSe NCs with a mixed ligand shell of octanoic acid and oleic acid (C8/OA-CdSe)

https://doi.org/10.1021/acs.jpclett.2c00514
J. Phys. Chem. Lett. 2022, 13, 3002−3007

directly dissolved in 3 mM DPA/toluene solution, as efforts to synthesize pure C8-CdSe with hot injection methods failed in our hands. Despite missing the 9ACA transmitter, direct energy transfer from C8/OA-CdSe to DPA resulted in a relatively high UCQY of 6.94% (Figure 4). This UCQY is

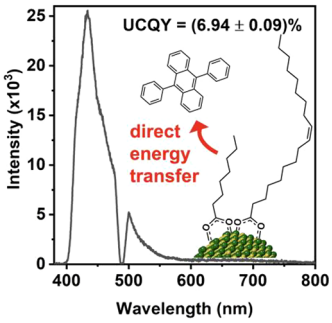

Figure 4. Upconversion photoluminescence spectra of C8/OA-CdSe in DPA/toluene solution under 488 nm excitation at RT. CdSe NCs with a mixed ligand shell of octanoic acid and oleic acid (C8/OA-CdSe) were directly dissolved in 3 mM DPA/toluene solution. Upconversion luminescence is observed at 430 nm with UCQY = (6.94 ± 0.09)%, showing the direct energy transfer from QDs to the emitter without 9-ACA transmitter ligands.

comparable to the 18.1% from the OA-CdSe/9ACA and 2 orders of magnitude higher than pristine OA-CdSe that has no 9ACA.[1] However, this mixed ligand shell is not colloidally stable, and over time, the UCQY dropped to 3−4% as the NC trap state emission increased at the expense of TET from CdSe to DPA (see Figure S3). Nonetheless, this data shows it is possible to directly transfer triplet excitons efficiently from NC donors to molecular acceptors in solution without 9-ACA transmitter ligands to achieve a high UCQY. It is important to point out that while short hexanoic acid ligands were used to increase TET in solid-state PbS NC-sensitized thin films to obtain a UCQY of 7%, the authors assumed that triplet transfer occurred through the aliphatic bridges.[23] Here we show that TET bypasses the short aliphatic ligands and direct TET occurs between CdSe and DPA.

A plot of the logarithm of the k_{TET2} rate as a function of carboxylic acid ligand length is shown in Figure 5. According to the Dexter energy transfer model,[15] the TET rate should decay exponentially with r, the donor−acceptor distance: $k_{TET} \propto e^{-\beta r}$.

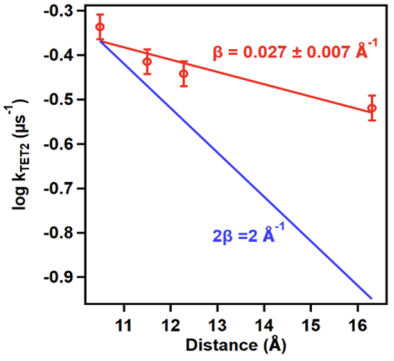

Figure 5. Rate constants of triplet energy transfer 2 (TET2) from the CdSe NC to emitter, per emitter (total rate divided by average number of bound 9-ACA mediator molecules). Plotted in the blue line is the rate vs distance curve with a 2 Å^{-1} slope for comparison.

An exponential fit of the k_{TET2} rate shown in Figure 4 leads to an exponential damping coefficient, β, of 0.027 ± 0.007 Å^{-1} (Figure 5). This weak distance dependence is very different when compared with charge transport through linear aliphatic ligands, assuming Dexter energy transfer involves a hole and an electron transfer step, and therefore, a steeper slope of two times the damping coefficient of electron transfer through an alkyl chain, a value of $2\beta \sim 2$ Å^{-1}, is expected.[24] This indicates that the TET process does not involve electron and hole tunneling through the aliphatic ligand. Indeed, it is also 20× lower than the damping coefficient of 0.52 Å^{-1} for aliphatic ligands for TET from PbS NCs to rubrene in photon upconverting thin films.[23] In order to rationalize this, we hypothesize that DPA acceptor molecules have to come into close contact with 9-ACA, within the Dexter distance of 1 nm[15] and at proper molecular orientation to enable strong orbital overlap to accept triplet excitons. The ligand length dependence reflects the accessibility of the surface adsorbed 9-ACA by DPA in solution. A similar conclusion has been shown in a previous study.[25] Besides, the carboxylic acid ligand surface packing geometry also modifies the accessibilty of the 9-ACA transmitter ligand for the TET2 process.[26] A recent study of electron transfer from QDs capped with mercapto-carboxylic acid of different lengths (or the number of methylene units, n) shows that the accessibility of QD surface sites by redox mediators increases abruptly at $n < 7$ ligands (similar to the length of C8 ligand used here) because of more disorder in capping ligand structure with short chain lengths.[27] We hypothesize that similar changes in ligand order may be responsible for observed length dependence of TET2 rates in this photon upconversion system.

CONCLUSION

This is the first time efficient QD-based photon upconversion up to 6.94% is achieved without a transmitter ligand (9ACA) where short octanoic acid ligands enable direct TET2 from CdSe QDs to the DPA emitters. This work shows that short capping ligands on QDs enable direct TET from the QD triplet photosensitizer to the triplet acceptor in solution, bypassing the adsorbed mediator ligand. This understanding will enable the design of oil-in-water micelles for QD-based photon upconversion. It provides guidance for the design of QD-based photocatalysts or light absorbers for solar photochemistry or imaging applications. This work also shows that k_{TET2} is 3 orders of magnitude below the diffusion limited rate, which implies that not every collision of 9-ACA with DPA results in successful TET, since both donor and acceptor must be in close contact and have strong molecular orbital overlap for efficient Dexter energy transfer. The design of molecules with improved intermolecular TET efficiency would also improve triplet−triplet annihilation quantum yields and thus the overall yield of photon upconversion.

ASSOCIATED CONTENT

Supporting Information

The Supporting Information is available free of charge at https://pubs.acs.org/doi/10.1021/acs.jpclett.2c00514.

Experimental methods, synthesis, and data fitting procedures (PDF)

https://doi.org/10.1021/acs.jpclett.2c00514
J. Phys. Chem. Lett. 2022, 13, 3002−3007

AUTHOR INFORMATION

Corresponding Authors

Tianquan Lian − *Department of Chemistry, Emory University, Atlanta, Georgia 30322, United States;* orcid.org/0000-0002-8351-3690; Email: tlian@emory.edu

Ming Lee Tang − *Department of Chemistry, University of Utah, Salt Lake City, Utah 84112, United States; Department of Materials Science and Engineering and Department of Chemistry, University of California, Riverside, Riverside, California 92521, United States;* orcid.org/0000-0002-7642-2598; Email: minglee.tang@utah.edu

Zihao Xu − *Department of Chemistry, Emory University, Atlanta, Georgia 30322, United States;* orcid.org/0000-0003-0805-8533; Email: zihao.xu@emory.edu

Authors

Tsumugi Miyashita − *Department of Biomedical Engineering, University of Utah, Salt Lake City, Utah 84112, United States; Department of Bioengineering, University of California, Riverside, Riverside, California 92521, United States;* orcid.org/0000-0003-0280-9148

Paulina Jaimes − *Department of Chemistry, University of Utah, Salt Lake City, Utah 84112, United States; Department of Materials Science and Engineering, University of California, Riverside, Riverside, California 92521, United States*

Complete contact information is available at: https://pubs.acs.org/10.1021/acs.jpclett.2c00514

Notes

The authors declare no competing financial interest.

ACKNOWLEDGMENTS

M.L.T. acknowledges the financial support by the U.S. Department of Energy, Office of Science, Office of Basic Energy Sciences, Solar Photochemistry Program under Award Number (DE-SC0022523). T.L. acknowledges the financial support from the National Science Foundation (CHE-2004080). The authors declare no conflict of interest.

REFERENCES

(1) Huang, Z. Y.; Li, X.; Mahboub, M.; Hanson, K. M.; Nichols, V. M.; Le, H.; Tang, M. L.; Bardeen, C. J. Hybrid Molecule-Nanocrystal Photon Upconversion Across the Visible and Near-Infrared. *Nano Lett.* **2015**, *15* (8), 5552−5557.

(2) Mongin, C.; Garakyaraghi, S.; Razgoniaeva, N.; Zamkov, M.; Castellano, F. N. Direct observation of triplet energy transfer from semiconductor nanocrystals. *Science* **2016**, *351* (6271), 369−372.

(3) Wu, M. F.; Congreve, D. N.; Wilson, M. W. B.; Jean, J.; Geva, N.; Welborn, M.; Van Voorhis, T.; Bulovic, V.; Bawendi, M. G.; Baldo, M. A. Solid-state infrared-to-visible upconversion sensitized by colloidal nanocrystals. *Nat. Photonics* **2016**, *10* (1), 31−34. Amemori, S.; Gupta, R. K.; Bohm, M. L.; Xiao, J.; Huynh, U.; Oyama, T.; Kaneko, K.; Rao, A.; Yanai, N.; Kimizuka, N. Hybridizing semiconductor nanocrystals with metal-organic frameworks for visible and near-infrared photon upconversion. *Dalton Trans* **2018**, *47* (26), 8590−8594.

(4) Tayebjee, M. J. Y.; McCamey, D. R.; Schmidt, T. W. Beyond Shockley-Queisser: Molecular Approaches to High-Efficiency Photovoltaics. *J. Phys. Chem. Lett.* **2015**, *6* (12), 2367−2378.

(5) Chen, S.; Weitemier, A. Z.; Zeng, X.; He, L. M.; Wang, X. Y.; Tao, Y. Q.; Huang, A. J. Y.; Hashimotodani, Y.; Kano, M.; Iwasaki, H.; et al. Near-infrared deep brain stimulation via upconversion nanoparticle-mediated optogenetics. *Science* **2018**, *359* (6376), 679−683. Lin, X. D.; Chen, X.; Zhang, W. C.; Sun, T. Y.; Fang, P. L.; Liao, Q. H.; Chen, X.; He, J. F.; Liu, M.; Wang, F.; et al. Core-Shell-Shell Upconversion Nanoparticles with Enhanced Emission for Wireless Optogenetic Inhibition. *Nano Lett.* **2018**, *18* (2), 948−956.

(6) Xu, Z. H.; Huang, Z. Y.; Li, C. Y.; Huang, T. T.; Evangelista, F. A.; Tang, M. L.; Lian, T. Q. Tuning the Quantum Dot (QD)/Mediator Interface for Optimal Efficiency of QD-Sensitized Near-Infrared-to-Visible Photon Upconversion Systems. *ACS Appl. Mater. Interfaces* **2020**, *12* (32), 36558−36567.

(7) Schmidt, T. W.; Castellano, F. N. Photochemical Upconversion: The Primacy of Kinetics. *J. Phys. Chem. Lett.* **2014**, *5* (22), 4062−4072.

(8) Huang, Z. Y.; Li, X.; Yip, B. D.; Rubalcava, J. M.; Bardeen, C. J.; Tang, M. L. Nanocrystal Size and Quantum Yield in the Upconversion of Green to Violet Light with CdSe and Anthracene Derivatives. *Chem. Mater.* **2015**, *27* (21), 7503−7507. Mahboub, M.; Maghsoudiganjeh, H.; Pham, A. M.; Huang, Z. Y.; Tang, M. L. Triplet Energy Transfer from PbS(Se) Nanocrystals to Rubrene: the Relationship between the Upconversion Quantum Yield and Size. *Adv. Funct. Mater.* **2016**, *26* (33), 6091−6097. Xia, P.; Raulerson, E. K.; Coleman, D.; Gerke, C. S.; Mangolini, L.; Tang, M. L.; Roberts, S. T. Achieving spin-triplet exciton transfer between silicon and molecular acceptors for photon upconversion. *Nat. Chem.* **2020**, *12* (2), 137−144.

(9) Rigsby, E. M.; Miyashita, T.; Jaimes, P.; Fishman, D. A.; Tang, M. L. On the size-dependence of CdSe nanocrystals for photon upconversion with anthracene. *J. Chem. Phys.* **2020**, *153* (11), 5.

(10) Huang, Z. Y.; Xu, Z. H.; Mahboub, M.; Liang, Z. M.; Jaimes, P.; Xia, P.; Graham, K. R.; Tang, M. L.; Lian, T. Q. Enhanced Near-Infrared-to-Visible Upconversion by Synthetic Control of PbS Nanocrystal Triplet Photosensitizers. *J. Am. Chem. Soc.* **2019**, *141* (25), 9769−9772.

(11) Huang, Z. Y.; Tang, M. L. Designing Transmitter Ligands That Mediate Energy Transfer between Semiconductor Nanocrystals and Molecules. *J. Am. Chem. Soc.* **2017**, *139* (28), 9412−9418. Huang, Z. Y.; Simpson, D. E.; Mahboub, M.; Li, X.; Tang, M. L. Ligand enhanced upconversion of near-infrared photons with nanocrystal light absorbers. *Chem. Sci.* **2016**, *7* (7), 4101−4104.

(12) De Roo, J.; Huang, Z. Y.; Schuster, N. J.; Hamachi, L. S.; Congreve, D. N.; Xu, Z. H.; Xia, P.; Fishman, D. A.; Lian, T. Q.; Owen, J. S.; et al. Anthracene Diphosphate Ligands for CdSe Quantum Dots; Molecular Design for Efficient Upconversion. *Chem. Mater.* **2020**, *32* (4), 1461−1466.

(13) Yonemoto, D. T.; Papa, C. M.; Mongin, C.; Castellano, F. N. Thermally Activated Delayed Photoluminescence: Deterministic Control of Excited-State Decay. *J. Am. Chem. Soc.* **2020**, *142* (25), 10883−10893.

(14) Xia, P.; Schwan, J.; Dugger, T. W.; Mangolini, L.; Tang, M. L. Air-Stable Silicon Nanocrystal-Based Photon Upconversion. *Adv. Opt. Mater.* **2021**, *9* (17), 6. Sanders, S. N.; Gangishetty, M. K.; Sfeir, M. Y.; Congreve, D. N. Photon Upconversion in Aqueous Nanodroplets. *J. Am. Chem. Soc.* **2019**, *141* (23), 9180−9184.

(15) Dexter, D. L. A THEORY OF SENSITIZED LUMINESCENCE IN SOLIDS. *J. Chem. Phys.* **1953**, *21* (5), 836−850.

(16) Morris-Cohen, A. J.; Malicki, M.; Peterson, M. D.; Slavin, J. W. J.; Weiss, E. A. Chemical, Structural, and Quantitative Analysis of the Ligand Shells of Colloidal Quantum Dots. *Chem. Mater.* **2013**, *25* (8), 1155−1165. Knowles, K. E.; Malicki, M.; Weiss, E. A. Dual-Time Scale Photoinduced Electron Transfer from PbS Quantum Dots to a Molecular Acceptor. *J. Am. Chem. Soc.* **2012**, *134* (30), 12470−12473.

(17) Olshansky, J. H.; Harvey, S. M.; Pennel, M. L.; Krzyaniak, M. D.; Schaller, R. D.; Wasielewski, M. R. Using Photoexcited Core/Shell Quantum Dots To Spin Polarize Appended Radical Qubits. *J. Am. Chem. Soc.* **2020**, *142* (31), 13590−13597.

(18) Fritzinger, B.; Capek, R. K.; Lambert, K.; Martins, J. C.; Hens, Z. Utilizing Self-Exchange To Address the Binding of Carboxylic Acid Ligands to CdSe Quantum Dots. *J. Am. Chem. Soc.* **2010**, *132* (29), 10195−10201.

(19) Gomes, R.; Hassinen, A.; Szczygiel, A.; Zhao, Q. A.; Vantomme, A.; Martins, J. C.; Hens, Z. Binding of Phosphonic Acids to CdSe Quantum Dots: A Solution NMR Study. *J. Phys. Chem. Lett.* **2011**, *2* (3), 145−152.
(20) Weir, M. P.; Toolan, D. T. W.; Kilbride, R. C.; Penfold, N. J. W.; Washington, A. L.; King, S. M.; Xiao, J.; Zhang, Z. L.; Gray, V.; Dowland, S.; et al. Ligand Shell Structure in Lead Sulfide-Oleic Acid Colloidal Quantum Dots Revealed by Small-Angle Scattering. *J. Phys. Chem. Lett.* **2019**, *10* (16), 4713−4719. Geva, N.; Shepherd, J. J.; Nienhaus, L.; Bawendi, M. G.; Van Voorhis, T. Morphology of Passivating Organic Ligands around a Nanocrystal. *J. Phys. Chem. C* **2018**, *122* (45), 26267−26274.
(21) Zhu, H. M.; Yang, Y.; Wu, K. F.; Lian, T. Q. Charge Transfer Dynamics from Photoexcited Semiconductor Quantum Dots. *Annu. Rev. Phys. Chem.* **2016**, *67*, 259−281.
(22) Huang, Z. Y.; Xia, P.; Megerdich, N.; Fishman, D. A.; Vullev, V. I.; Tang, M. L. ZnS Shells Enhance Triplet Energy Transfer from CdSe Nanocrystals for Photon Upconversion. *ACS Photonics* **2018**, *5* (8), 3089−3096.
(23) Nienhaus, L.; Wu, M. F.; Geva, N.; Shepherd, J. J.; Wilson, M. W. B.; Bulovic, V.; Van Voorhis, T.; Baldo, M. A.; Bawendi, M. G. Speed Limit for Triplet-Exciton Transfer in Solid-State PbS Nanocrystal-Sensitized Photon Upconversion. *ACS Nano* **2017**, *11* (8), 7848−7857.
(24) Closs, G. L.; Miller, J. R. INTRAMOLECULAR LONG-DISTANCE ELECTRON-TRANSFER IN ORGANIC-MOLECULES. *Science* **1988**, *240* (4851), 440−447. Beratan, D. N. ELECTRON-TUNNELING THROUGH RIGID MOLECULAR BRIDGES - BICYCLO 2.2.2 OCTANE. *J. Am. Chem. Soc.* **1986**, *108* (15), 4321−4326. Lai, R.; Liu, Y.; Luo, X.; Chen, L.; Han, Y.; Lv, M.; Liang, G.; Chen, J.; Zhang, C.; Di, D.; et al. Shallow distance-dependent triplet energy migration mediated by endothermic charge-transfer. *Nat. Commun.* **2021**, *12* (1), 1532. Engelkes, V. B.; Beebe, J. M.; Frisbie, C. D. Length-Dependent Transport in Molecular Junctions Based on SAMs of Alkanethiols and Alkanedithiols: Effect of Metal Work Function and Applied Bias on Tunneling Efficiency and Contact Resistance. *J. Am. Chem. Soc.* **2004**, *126* (43), 14287−14296.
(25) Hartmann, L.; Kumar, A.; Welker, M.; Fiore, A.; Julien-Rabant, C.; Gromova, M.; Bardet, M.; Reiss, P.; Baxter, P. N. W.; Chandezon, F.; et al. Quenching Dynamics in CdSe Nanoparticles: Surface-Induced Defects upon Dilution. *ACS Nano* **2012**, *6* (10), 9033−9041.
(26) De Nolf, K.; Cosseddu, S. M.; Jasieniak, J. J.; Drijvers, E.; Martins, J. C.; Infante, I.; Hens, Z. Binding and Packing in Two-Component Colloidal Quantum Dot Ligand Shells: Linear versus Branched Carboxylates. *J. Am. Chem. Soc.* **2017**, *139* (9), 3456−3464.
(27) Yang, W. X.; Vansuch, G. E.; Liu, Y. W.; Jin, T.; Liu, Q. L.; Ge, A. M.; Sanchez, M. L. K.; Haja, D. K.; Adams, M. W. W.; Dyer, R. B.; et al. Surface-Ligand "Liquid" to "Crystalline" Phase Transition Modulates the Solar H-2 Production Quantum Efficiency of CdS Nanorod/Mediator/Hydrogenase Assemblies. *ACS Appl. Mater. Interfaces* **2020**, *12* (31), 35614−35625.

https://doi.org/10.1021/acs.jpclett.2c00514
J. Phys. Chem. Lett. 2022, 13, 3002−3007